



ChemComm

**A Single Carbon Atom Controls Geometry and Reactivity of  
CoII(N<sub>2</sub>S<sub>2</sub>) Complexes**

Journal:	<i>ChemComm</i>
Manuscript ID	CC-COM-11-2023-005394.R1
Article Type:	Communication

SCHOLARONE™  
Manuscripts

# A Single Carbon Atom Controls Geometry and Reactivity of $\text{Co}^{\text{II}}(\text{N}_2\text{S}_2)$ Complexes

Received 00th January 20xx,  
Accepted 00th January 20xx

Manish Jana,<sup>a</sup> Manuel Quiroz<sup>a</sup> and Marcetta Y. Darensbourg<sup>\*a</sup>

DOI: 10.1039/x0xx00000x

**Three- vs two-carbon N-to-N connectors give rise to monomeric, tetrahedral  $\text{N}_2\text{S}_2\text{Co}(\text{II})$  ( $\mu_{\text{eff}} = 4.24 \text{ BM}$ ) or dimeric  $[(\text{N}_2\text{S}_2)\text{Co}(\text{II})]_2$  (diamagnetic) complexes respectively. Differences in derivative products of Lewis Acid receivers,  $\text{W}^0(\text{CO})_3$  Or  $\text{W}^0(\text{CO})_4$ , illustrate nucleophilicity of the thiolate sulfur lone pairs in each case, as well as their structural control.**

The vast synthetic design space encompassed by  $\text{MN}_2\text{S}_2$  complexes includes variations in metal and hydrocarbon connectors, specifically in the N-to-N and S-to-S linkages. This diverse array of combinations, influenced by the nucleophilicity of well-oriented cis dithiolates, has given rise to a multitude of S-bridged, hetero bi- and polymetallic complexes. Such  $\text{MN}_2\text{S}_2$  serve as metallothiolate ligands, and, when  $M = \text{Ni}$ , serve as biomimetics for the tight binding Cys-X-Cys tripeptide site of Ni(II) in the dinickel Acetyl CoA Synthase (ACS) bioorganometallic catalyst. For Nitrile Hydratase (NHase), the monomeric  $\text{MN}_2\text{S}_2$  complexes take the form of  $M = \text{Fe}$  or  $\text{Co}$ , post-translationally modified by oxygenation at sulfur.<sup>1</sup>

The requirement of contiguous SNNS donor sites conforming to a square plane has inspired efforts to contrast the three 3d metal ions  $M = \text{Ni}^{2+}$ ,  $[\text{Fe}(\text{NO})]^{2+}$ , and  $[\text{Co}(\text{NO})]^{2+}$  enclosed in identical  $\text{N}_2\text{S}_2$  tetradentate binding sites. Synthetic results indicate that the robust Ni(II) $\text{N}_2\text{S}_2$  is the most predictably reliable synthon as a metallothiolate ligand to an exogenous metal. The  $[\text{Fe}(\text{NO})]\text{N}_2\text{S}_2$  offers an additional advantage with its distinctive  $\nu(\text{NO})$  vibrational signature, EPR-active  $S = \frac{1}{2}$  signal, and accessible reduction potential.<sup>2</sup> Limited information is available for  $M = \text{Co}(\text{II})$  or  $\text{Co}(\text{III})(\text{NO})^-$ , owing to its chemical non-innocence (volatility) involving NO transfer, sometimes accompanied by Co exchange with other metals or uptake of solvent donors, resulting in intricate and unpredictable formulations.<sup>3</sup>

Achieving a square planar orientation in  $\text{N}_2\text{S}_2$  ligands necessitates a delicate balance between metal d-orbital preferences and the dihedral angle requirements of hydrocarbon linkers (N to N or N to S). In this context, cobalt derivatives, with diverse coordination numbers and structures, emerge as prime paradigms for understanding these fundamental properties. Cobalt(II) complexes also stand out for

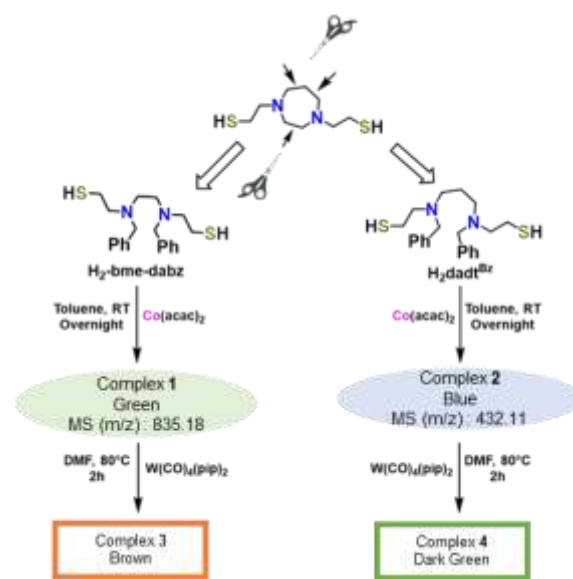


Fig. 1 Synthetic scheme for complexes of this study.

their typically large magnetic anisotropy, making them valuable for the development of small molecular magnets. This magnetic anisotropy primarily originates from spin-orbit coupling, a phenomenon strategically regulated by geometry and coordination environment.<sup>4</sup>

This focus has directed us to target and develop a di-benzylated  $\text{N}_2\text{S}_2$  ligand, where the nitrogens are connected by two and three carbons, resulting in two types of  $\text{MN}_2\text{S}_2$  products: dimeric and monomeric, respectively. The ability of these new  $[\text{CoN}_2\text{S}_2]$  metallo-ligands to capture exogenous metals is demonstrated using a classic redox-innocent receiver and spectroscopic probe synthon, (piperidine)<sub>2</sub> $\text{W}(\text{CO})_4$ .<sup>5</sup> This communication outlines the inaugural results of our investigation into this system.

Fig. 1 describes the synthesis and isolation of complexes **1** and **2**, and their reactions with (pip)<sub>2</sub> $\text{W}(\text{CO})_4$ . Reaction of  $\text{H}_2\text{bme-dabz}$  (2,2'-(ethane-1,2-diylbis(benzylazanediy))bis(ethane-1-thiol); a 2-carbon linker is between the nitrogens) ligand with cobalt acetylacetonate  $[\text{Co}^{\text{II}}(\text{acac})_2]$  in toluene yielded a green powder over the course of 4h at RT, which was isolated via filtration. The green solid product **1**, was insoluble in almost all organic solvents at RT.

A similar reaction of the  $\text{H}_2\text{-dadt}^{\text{Bz}}$  (2,2'-(propane-1,3-diylbis(benzylazanediy))bis(ethane-1-thiol), 3-carbon linker

<sup>a</sup> Department of Chemistry, Texas A&M University, College Station, Texas-77843, US.

† Footnotes relating to the title and/or authors should appear here.

Electronic Supplementary Information (ESI) available: [details of any supplementary information available should be included here]. See DOI: 10.1039/x0xx00000x

between the nitrogens) ligand with cobalt acetylacetonate in toluene produced a blue, rather than green, solid.

The blue solid is readily soluble in polar organic solvents such as DCM, MeCN, DMF etc. The APCI-MS (atmospheric pressure chemical ionization mass spectrometry) for the green solid in DMF/MeCN mixture showed a parent signal at  $m/z = 418.0928$  along with another small peak at  $m/z = 835.18$  for complex **1** (Fig. S1). In contrast, the blue product, complex **2** in DCM was blank in the  $m/z = 850-900$  region of the mass spectrometry, but instead a peak at  $m/z = 432.11$  was observed (Fig. S3). The mass spectrum analysis indicates that complex **1** is likely dimeric in solution similarly to the previously reported diiron complexes using  $N_2S_2$  ligands,<sup>6</sup> and thus, a similar formulation was expected for the cobalt analogues. However, the mass spectrometric result for the blue product **2**, is consistent with a monomeric form in solution.

Cyclic voltamographic scans of complexes **1** and **2** were carried out in DMF (Fig. S16 and Fig. S18). Complex **1** shows an event assigned to the Co(II)/Co(III) couple at  $-0.65$  V in the anodic scan, whereas complex **2** shows a similar irreversible oxidation event at  $-0.37$  V. A simple explanation is that the more positive oxidation potential of complex **2** derives from a more electron-rich ligand field, or first coordination sphere, which should stabilize the higher oxidation state.

To further probe the properties of  $MN_2S_2$  complexes, the donating ability of such metallodithiolates as ligands in adducts of  $W(CO)_4$  derived from labile bis piperidine ligands was examined. The formation of  $MN_2S_2 \cdot W(CO)_4$  utilizes the sulfur electron density through thiolate-bridging to the metal carbonyl Lewis acid receiver complex. The  $\nu(CO)$  vibrational probe is a well-established approach for comparing classical ligands such as phosphines and bipyridines, and we have ranked the electron-donating ability of *cis*-dithiolate complexes as ligands as well.<sup>7</sup> The reactions of complexes **1** and **2** with  $[W(CO)_4(pip)_2]$  were carried out in DMF at  $80^\circ C$  for 2h. The color of the final products as well as the FTIR in the  $\nu(CO)$  reporter ligands region, Fig. 2, showed a clear difference between two products. The IR pattern for Complex **3** is similar to that observed for four CO ligands in  $C_{2v}$  symmetry as is typical for metallodithiolate derivatives of  $W(CO)_4$  (Table S5). In contrast, the 2-band pattern seen for Complex **4** (in DMF) appears as a pseudo  $C_{3v}$  pattern, originating from asymmetric ligation. Its interpretation follows the discussion of XRD structural results.

Complex **1**, sparingly soluble in hot DMF, underwent recrystallization from a hot DMF and ether mixture, yielding dark green crystals. Complex **2** resulted from crystallization of the blue solid in DCM with hexane layering. Complexes **3** and **4** crystallize via vapor diffusion of diethyl ether into a concentrated DMF solution over 3-4 days. Complex **3** forms brown needles, while Complex **4** yields brownish-green, block-shaped crystals.

From single crystal XRD analysis, the molecular structures of  $[Co(bme-dabz)]_2$  (**1**),  $Co(dadt^{Bz})$  (**2**),  $\{[(bme-dabz)Co(DMF)] \cdot W(CO)_4\}$  (**3**) and  $\{[(dadt^{Bz})Co(DMF)]_2 \cdot \{W(CO)_3\}_2\}$  (**4**) are as shown in Fig. 3, 50% probability thermal ellipsoid plots; selected metric parameters are tabulated within Fig. 3.

Complexes **1** and **2** crystallize in monoclinic  $I2/a$  and

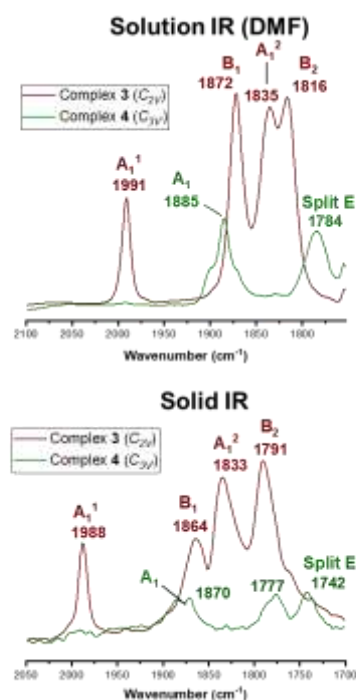


Fig. 2.  $\nu(CO)$  solution (DMF) and solid (ATR) IR spectra of complex **3** and **4**; assignments according to their symmetries from XRD analysis.

orthorhombic  $Pbca$  space groups respectively. The crystal structure of **1** shows that both the cobalt centers of the dimeric structure adopt a severely distorted square pyramidal geometry with  $\tau_5$  values of 0.44. The two cobalt centers of **1** form a  $Co_2S_2$  diamond core; the distance between the cobalt centers (within the core) is  $3.226 \text{ \AA}$ . The  $\angle S-Co-S$  angle (within the  $N_2S_2$  ligand field) is found to be  $96.84^\circ$  while the  $\angle N-Co-N$  angle is  $80.21^\circ$ .

In contrast to **1**, the single crystal X-ray diffraction analysis of **2** reveals a monomeric, tetrahedral cobalt complex. The cobalt center adopts a distorted tetrahedral geometry ( $\tau_4 = 0.77$ ) with the  $\angle S-Co-S$  angle of  $126.9^\circ$  and the  $\angle N-Co-N$  angle of  $104.36^\circ$ . As far as we know, this is the first reported tetrahedral Co(II) complex in an  $N_2S_2$  ligand field.

The dark brown, needle-shaped crystals obtained for complex **3** belong to the monoclinic  $P21/c$  space group. The connection of the  $(N_2S_2)Co$  unit to  $W(CO)_4$  creates an octahedral geometry at tungsten with a  $\angle S-W-S$  angle of ca.  $81^\circ$ . The residual lone pair of each sulfur generates a hinge in the bridge between the two metals, whose angle of ca.  $116.7^\circ$  is defined as the dihedral angle between the  $N_2S_2$  and  $S_2W(CO)_2$  best planes. The cobalt center in the  $N_2S_2$  pocket of  $\{[(bme-dabz)Co(DMF)] \cdot W(CO)_4\}$  (complex **3**), adopts almost ideal square pyramidal geometry with  $\tau_5 = 0.07$ ; where the fifth coordination site is fulfilled by apical DMF coordination. The displacement of the cobalt from the mean  $N_2S_2$  plane is  $0.596 \text{ \AA}$ . At  $3.334 \text{ \AA}$ , the distance between Co-W is beyond bonding.

Reaction of complex **2** with  $(pip)_2W(CO)_4$  yielded complex **4**, a tetranuclear,  $Co_2W_2$ , complex. Complex **4** crystallizes in the monoclinic  $P21/n$  space group. The cobalt centers inside the  $N_2S_2$  pockets adopt distorted square pyramidal geometry with a ligated DMF molecule at the apical position having  $\tau_5$  values of

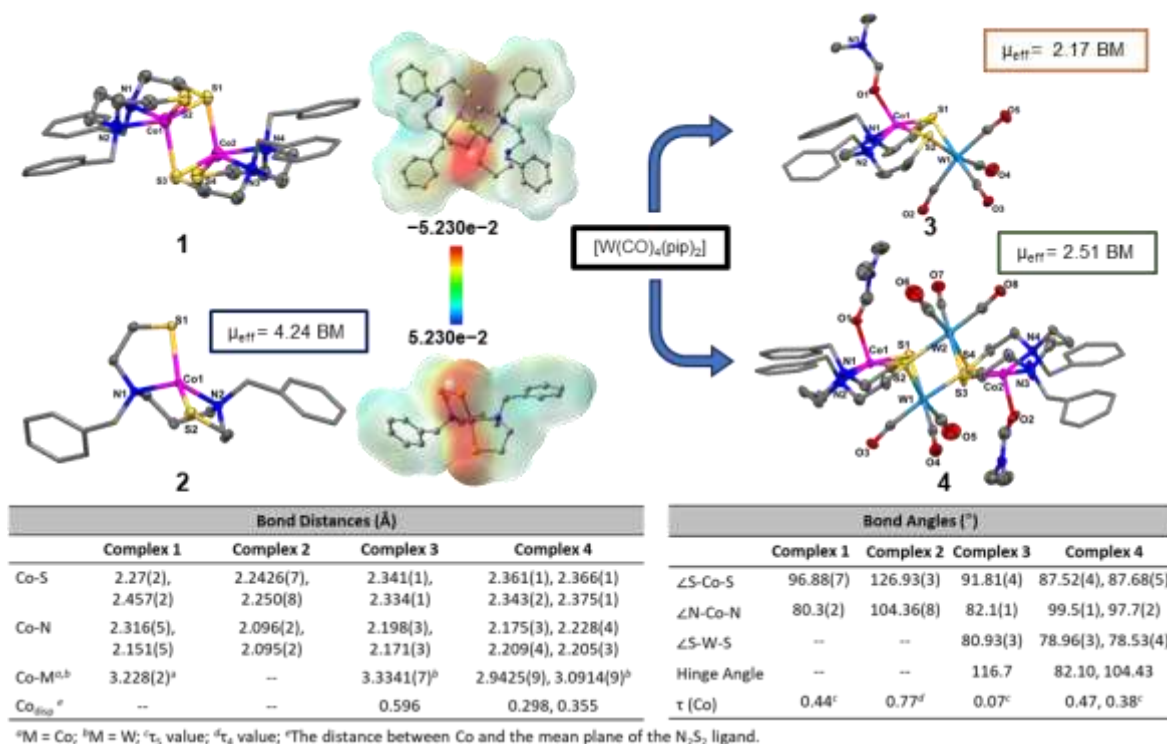


**Fig. 3** Single crystal x-ray structures of complexes **1**, **2**, **3** and **4** showing 50% probability thermal ellipsoid plots. Hydrogen atoms are omitted for clarity. The benzene rings are shown as sticks. Selected bond distances and angles are listed in the imbedded table.

0.47 and 0.38. One sulfur from the CoN<sub>2</sub>S<sub>2</sub> ligand serves as a simple  $\mu_2$ -bridge to W(CO)<sub>3</sub> while the second sulfur bridges two W(CO)<sub>3</sub> units. Thus, the octahedral coordination sphere of W is completed by different types of S-bridges yielding  $\mu$ -S<sub>2</sub>W(CO)<sub>3</sub> units. The Co-W distances for complex **4** are found to be 2.94 and 3.09 Å respectively, relatively smaller than that of complex **3**. The displacement of the cobalt centers from the mean N<sub>2</sub>S<sub>2</sub> plane is also found to be somewhat less (0.298 Å and 0.355 Å) as compared to complex **3**. The table in Fig. 3 contains metric parameters for complexes **1-4**.

The  $\nu(\text{CO})$  assignment for W(CO)<sub>4</sub> in solution are compatible with the XRD structure for complex **3**. The absorption bands for previously reported Fe, Co and Ni complexes<sup>6</sup> are listed in Table S5 with assignments according to the C<sub>2v</sub> symmetry of the W(CO)<sub>4</sub> moiety for comparison. As reported previously, the  $\nu(\text{CO})$  values are measures of electron density at the tungsten according to the typical  $\sigma$ -donor/ $\pi$ -back-bonding arguments; the sulfur donors of the metallodithiolate ligands are known to be better donors to W(CO)<sub>4</sub> than are piperidine ligands in (pip)<sub>2</sub>W(CO)<sub>4</sub>. Furthermore, it has been observed that the electron donor abilities of Ni, [Co-1'(NO)] and [Fe-1'(NO)] toward W(CO)<sub>4</sub> are slightly poorer than that found in complex **3**, while the previously reported dianionic [Ni(ema)]<sup>2-</sup> ligand donates more electron density to the W(CO)<sub>4</sub> reporter unit.<sup>7</sup> In comparison between the Co(NO) and the Co(DMF) metalloligand, the latter is found to be a stronger donor, as the nitrosyl ligand in the former can pull significant amount of electron density from the central metal via  $\pi$  back bonding interaction, thus making the Co into a Co(III) and the sulfurs less nucleophilic. The frequency calculation (IR) on the DFT

optimized structure of complex **3** is also consistent with the experimental  $\nu(\text{CO})$  IR spectra (Fig. S38).

Complex **4** in DMF shows two absorption bands at ca. 1885 and 1785 cm<sup>-1</sup> in the  $\nu(\text{CO})$  IR region (Fig. 2). Such pseudo-C<sub>3v</sub> asymmetric donor sites have been analyzed for mixed ligand systems in [W(CO)<sub>3</sub>(dppm)(PPh<sub>3</sub>)] as well as [W(CO)<sub>3</sub>(dppm)(Ph<sub>2</sub>PCH<sub>2</sub>P(O)Ph<sub>2</sub>)] (Table S6).<sup>8</sup> While three carbonyl stretches are expected for these types of molecules, the observation of only two bands in DMF is due to limitations of the solvent window. The solid-state  $\nu(\text{CO})$  IR of complex **4** (ATR) shows 3-bands at ca. 1870, 1777 and 1742 cm<sup>-1</sup> (Fig. S2, right, green spectra) which is consistent (peak separation) with the IR spectrum of a pseudo-C<sub>3v</sub> symmetric molecule but appearing at a much lower wavenumber as compared to the reported tungsten diphos derivatives.<sup>8</sup> The DFT computation (frequency calculation) also supports the experimentally observed  $\nu(\text{CO})$  IR spectrum for complex **4** (Fig. S40).

Due to very poor solubility of complex **1** in common organic solvents, its <sup>1</sup>H NMR spectrum was not determined. The <sup>1</sup>H NMR spectrum of Complex **2** indicated paramagnetism (Fig. S12) at room temperature (295 K). With exception of complex **1**, the solution magnetic moments for all complexes were determined by Evans method.<sup>9</sup> The magnetic moment for complex **2** in CDCl<sub>3</sub>,  $\mu_{\text{eff}} = 4.24$  BM (Fig. S13), signifies a high spin tetrahedral Co(II), S = 3/2 species in solution. In CDCl<sub>3</sub>, the measured  $\mu_{\text{eff}}$  for **3** (2.17 BM, Fig. S14) slightly exceeds the expected spin-only value of 1.97 BM ( $g = 2.26$  from EPR, Fig. S30) for a S = 1/2 Co(II) species, indicating unquenched angular momentum.<sup>10</sup> DFT computation also shows that the doublet spin state is lower in

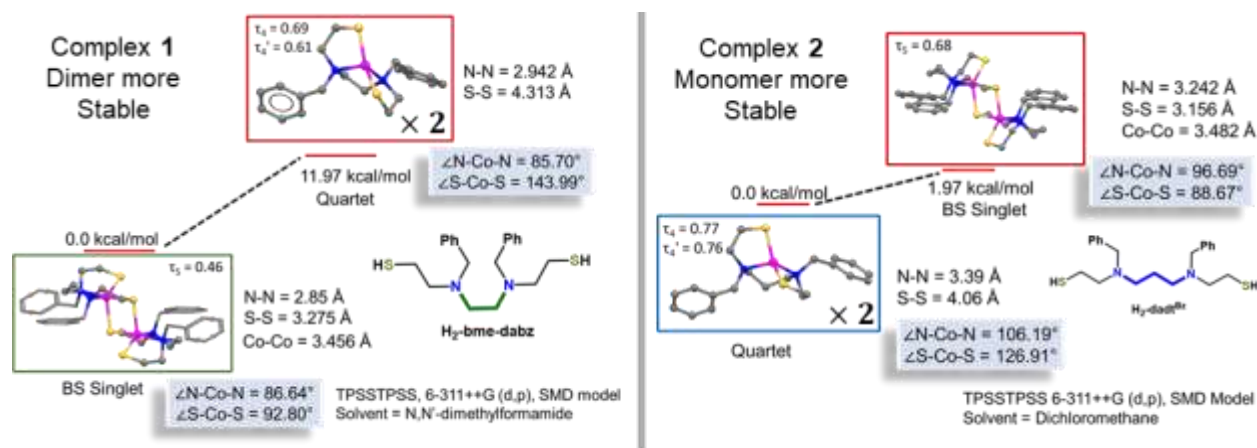


**Fig. 4** DFT computation of complex **1** (left) shows that the hypothetical monomer is of higher energy than that of the obtained dimeric cobalt complex. For complex **2** (right), DFT predict the hypothetical dimeric species to be higher in energy than the corresponding monomeric tetrahedral cobalt complex.

energy compared to the quartet state for complex **3** by 6.56 kcal/mol (Fig. S35). For complex **4**, the solution magnetic moment in DMSO- $d_6$  was found to be,  $\mu_{\text{eff}} = 2.52$  BM (Fig. S15), consistent with two uncoupled low spin Co(II),  $S = \frac{1}{2}$  spin centres (expected value is 2.45 BM for  $g = 2$ ).

The thermodynamic stabilities of **1** and **2** determined from DFT computations are shown in Fig. 4. The ground state energy difference ( $E_g$ ) for **1** between the dimeric vs two (hypothetical) monomeric tetrahedral cobalt structures (Fig. 4, left) reflect the thermodynamic stability of **1** in dimeric form (11.97 kcal/mol in favour of the dimeric structure). For **2**, the sum of two monomeric tetrahedral cobalt complexes is found to be 1.97 kcal/mol more stable than the corresponding hypothetical dimeric structure (Fig. 4, right). The calculated tetrahedral structure for **1** (top left, Fig. 4) shows greater deviation in bond angles (much larger  $\angle\text{S-Co-S}$  angle and much smaller  $\angle\text{N-Co-N}$  angle) than complex **2** (bond angles closer to  $109^\circ$ ) from an ideal tetrahedral structure. These parameters also reflect the thermodynamic stability of **1** and **2** in their respective dimeric and monomeric forms, i.e., the two-carbon N to N linker is more constrained.

In conclusion, this study provides a rare example of monomeric, tetrahedral Co complex in a  $\text{N}_2\text{S}_2$  ligand framework in which a single carbon atom between the N-to-N connector determines differences in structure and resultant reactivity. Tetrahedral cobalt(II) complexes have been the focus of several research groups, and are prized for their high magnetic anisotropy or zero field splitting parameters, some of which offer a large barrier height for magnetization reversal.<sup>4</sup> The greater nucleophilicity of the S in the monomeric complex gives rise to a  $\nu(\text{CO})$  pattern and position in the  $\text{W}(\text{CO})_3$  reporter group which is shifted to much lower wavenumbers compared to other reported pseudo  $\text{C}_{3v}$  structures. Future studies will be focused on detailed magnetic studies using solid state temperature dependent magnetic susceptibility measurements (SQUID) as well as high field EPR measurements for all the complexes.

This work was financially supported by the National Science Foundation (MPS CHE 2102159) and the Robert A. Welch

Foundation (A-0924). We acknowledge Dr. Yohanes H. Razenom for help with mass spectrometry. We are thankful to Prof. Donald J. Darensbourg and Prof. Michael B. Hall for their valuable insights on the infrared and computational studies, respectively.

## Conflicts of interest

There are no conflicts to declare.

## Notes and references

- (a) J. A. Denny and M. Y. Darensbourg, *Chem. Rev.*, 2015, **115**, 5248–5273. (b) M. Gennari and C. Duboc, *Acc. Chem. Res.*, 2020, **53**, 2753–2761.
- (a) C.-H. Hsieh, S. Ding, Ö. F. Erdem, D. J. Crouthers, T. Liu, C. C. L. McCrory, W. Lubitz, C. V. Popescu, J. H. Reibenspies, M. B. Hall and M. Y. Darensbourg, *Nat Commun*, 2014, **5**, 3684. (b) P. Ghosh, S. Ding, M. Quiroz, N. Bhuvanesh, C.-H. Hsieh, P. M. Palacios, B. S. Pierce, M. Y. Darensbourg and M. B. Hall, *Chem. Euro. J.*, 2018, **24**, 16003–16008.
- (a) P. Guerrero-Almaraz, M. Quiroz, J. H. Reibenspies and M. Y. Darensbourg, *Inorg. Chem.*, 2021, **60**, 15975–15979. (b) P. Guerrero-Almaraz, M. Quiroz, D. R. Rodriguez, M. Jana, M. B. Hall and M. Y. Darensbourg, *ACS Org. Inorg. Au*, DOI:10.1021/acsorginorgau.3c00025.
- (a) J. M. Zadrozny and J. R. Long, *J. Am. Chem. Soc.*, 2011, **133**, 20732–20734. (b) M. R. Saber and K. R. Dunbar, *Chem. Commun.*, 2014, **50**, 12266–12269. (d) Y. Rechkemmer, F. D. Breitgoff, M. van der Meer, M. Atanasov, M. Haki, M. Orlita, P. Neugebauer, F. Neese, B. Sarkar and J. van Slageren, *Nat Commun*, 2016, **7**, 10467. (e) S. Tripathi, S. Vaidya, K. U. Ansari, N. Ahmed, E. Rivière, L. Spillecke, C. Koo, R. Klingeler, T. Mallah, G. Rajaraman and M. Shannugam, *Inorg. Chem.*, 2019, **58**, 9085–9100. (f) C. M. Legendre, E. Damgaard-Møller, J. Overgaard and D. Stalke, *European Journal of Inorganic Chemistry*, 2021, **2021**, 3108–3114.
- D. J. Darensbourg and R. L. Kump, *Inorg. Chem.*, 1978, **17**, 2680–2682.
- H. N. Rabinowitz, K. D. Karlin and S. J. Lippard, *J. Am. Chem. Soc.*, 1977, **99**, 1420–1426.
- J. L. Hess, H. L. Conder, K. N. Green and M. Y. Darensbourg, *Inorg. Chem.*, 2008, **47**, 2056–2063.
- D. J. Darensbourg, D. J. Zalewski, C. Plepys and C. Campana, *Inorg. Chem.*, 1987, **26**, 3727–3732.
- D. F. Evans, *J. Chem. Soc.*, 1959, 2003–2005.
- (a) D. M. Jenkins, A. J. Di Bilio, M. J. Allen, T. A. Betley and J. C. Peters, *J. Am. Chem. Soc.*, 2002, **124**, 15336–15350. (b) O. Kahn, *Molecular magnetism*, Wiley-VCH, New York (N.Y.), 1993.